

DIRAC/PS212

CERN-EP-2020
November 15, 2020

DIRAC Collaboration status report to SPSC – October 2020

L. Nemenov (JINR) on behalf of the DIRAC Collaboration

1 K^+K^- pair analysis in the effective mass region near $2m_K$

The results of the experimental K^+K^- pair analysis in the effective mass region near two kaon masses were presented in the DIRAC annual report of October 2019. The data were analysed (Coulomb approach) proposing pointlike pair production and only Coulomb interaction in the final state (Fig.1(a)).

In the present report are shown the results of a more detailed investigation (several approaches) taking into account pointlike as well as nonpointlike K^+K^- pair generation with Coulomb and strong interaction in the final state (Fig.1(b)). In this analysis, three different theoretical models were used: Achasov, Martin and ALICE collaboration (see eg. [WPCF2019](https://www.wpcf2019.ch/dirac.web.cern.ch/DIRAC/WPCF2019.pdf) [dirac.web.cern.ch/DIRAC/WPCF2019.pdf]).

The experimental K^+K^- pair distributions were analysed by subtracting $\pi^+\pi^-$, $p\bar{p}$ and accidental pair backgrounds, using setup detectors and time-of-flight measurement. The residual background was evaluated and subtracted exploiting different dependence of K^+K^- and background pairs from Q . The complete analysis used a more precise description of the background than in the 2019 report.

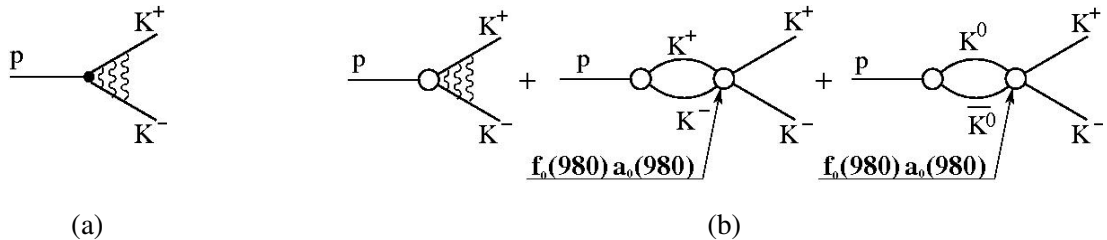


Fig. 1: K^+K^- production processes: a) pointlike production and Coulomb interaction in the final state, b) pointlike and nonpointlike pair generation with Coulomb and strong interaction in the final state.

1.1 Coulomb analysis

In the Coulomb analysis, the K^+K^- pair numbers were evaluated from the experimental Q_L and Q distributions which have different shapes.

In Fig.2 is shown the Q_L spectrum of the 70%, 50% and 30% subsamples for the RUNs 2009 and 2010. Each subsample was obtained by subtracting the background from the experimental distributions. Simulated distributions of K^+K^- pairs (Coulomb approach) and residual background of $\pi^+\pi^-$ and $p\bar{p}$ pairs are fitted to the experimental spectrum in the interval $0 < Q_L < 100 MeV/c$. The red line is the K^+K^- distribution and the black line the sum of K^+K^- and residual background. In the 70% and 30% subsamples, the residual background is small, and the lines coincide. For K^+K^- pairs in the Q_L region smaller than $10 MeV/c$, the Coulomb enhancement is clearly visible whereas the residual background is uniform.

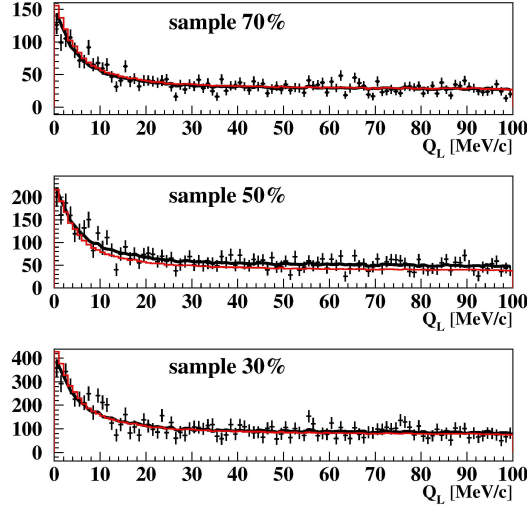


Fig. 2: Q_L distributions of the subsamples 30%, 50% and 70% for the RUNs 2009 and 2010. Simulated distributions of K^+K^- (Coulomb approach) and residual background of $\pi^+\pi^-$ and $p\bar{p}$ pairs are fitted to the experimental spectrum in the interval $0 < Q_L < 100\text{MeV}/c$. The red line is the K^+K^- distribution, the black line is the sum of K^+K^- and residual background. In the subsamples 70% and 30% the residual background is small and these lines practically coincide. For K^+K^- pairs in the region of $Q_L < 10\text{MeV}/c$, the Coulomb enhancement is clearly visible, whereas the residual background is uniform.

Table 1: Matching pair numbers for Q and Q_L distribution analyses. The errors of K^+K^- and background values are the same.

year	cut on ToF	distribution	K^+K^-	$\pi^+\pi^-$ & $p\bar{p}$ background
2009 + 2010	70%	Q	3900 ± 410	-110
		Q_L	3930 ± 580	-140
	50%	Q	5320 ± 730	1100
		Q_L	5460 ± 1020	960
	30%	Q	11220 ± 1370	180
		Q_L	10750 ± 2020	300

It is seen from Table 1 that the K^+K^- pair numbers, found in the Q and Q_L distributions, do not differ significantly.

1.2 Detailed analysis

The distributions in r^* , the relative distance between K^+ and K^- connecting K mesons from the decay of short-lived sources and long-lived resonances, are described by the sum: $w_g * Gauss + w_{K^*} * K^*(892) + w_\Lambda * \Lambda(1520) + w_\phi * \phi(1020)$.

The first term describes the contribution of the short-lived sources approximated by a Gaussian with the radius $r_0 \approx 1.5\text{fm}$, and the other terms describe the contributions of the three resonances. The w_i are the relative contributions of the different sources in K^+K^- pair production; the sum of w_i is equal to unity. The weight values and their errors were evaluated. The analysis was performed for three sets of w_i . The first extreme set (0.00, 0.76, 0.10, 0.14) maximises the contributions of $K^*(892)$, $\Lambda(1520)$ and $\phi(1020)$ resonances producing the largest value of the average r^* . The third extreme set (0.57, 0.35, 0.06, 0.02)

maximises the role of the short-lived K^+K^- pair sources generating the minimum value of the average r^* , and the second set (0.10, 0.76, 0.08, 0.06) uses intermediate values of w_i .

The distributions in Q (fitting curves) were calculated for each year and each set, using the three theoretical approaches of Achasov, Martin and ALICE. The experimental data of the 70% subsample were analysed by a dedicated fitting curve with $\pi^+\pi^-$ and $p\bar{p}$ background. The results are shown in Table 2. The difference between the extreme yield values gives the maximum systematic errors in connection with the uncertainty of the r^* distribution. The maximum error values are ± 70 , ± 55 and ± 40 . These systematic errors are significantly smaller than the errors in Table 2. Therefore, the other two experimental subsamples were analysed using only the intermediate distribution on r^* . In Table 2, the results for the 70%, 50% and 30% subsamples are summarised. One sees that the Achasov approach gives for any subsample a larger residual background deviation from zero than the Martin and ALICE approaches. The large level of residual background can be considered as the result of insufficient accuracy of the fitting curve describing the K^+K^- distribution in Q .

Table 2: Evaluated numbers of K^+K^- pairs for the three subsamples (70%, 50% and 30%), using different approaches.

	Achasov K^+K^- (backgr.)	Martin K^+K^- (backgr.)	ALICE K^+K^- (backgr.)	Total events
70% sample				3790
maximum r^*	3190 ± 330	3650 ± 370	3720 ± 380	
intrmediate r^*	3120 ± 320 (670)	3600 ± 360 (190)	3680 ± 370 (110)	
χ^2 2010/2009	1.03/1.20	1.00/1.18	1.00/1.18	
minimum r^*	3050 ± 320	3540 ± 360	3640 ± 370	
50% sample				6420
intrmediate r^*	4340 ± 570 (2080)	4940 ± 640 (1480)	5040 ± 660 (1380)	
χ^2 2010/2009	0.80/1.04	0.79/1.04	0.78/1.05	
30% sample				11030
intermediate r^*	9230 ± 1080 (1800)	10500 ± 1220 (530)	10680 ± 1240 (350)	
χ^2 2010/2009	0.70/0.89	0.68/0.88	0.68/0.88	

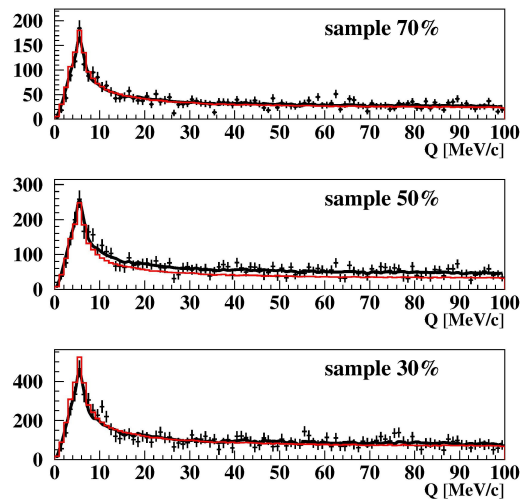


Fig. 3: Q distributions of the subsamples 30%, 50% and 70% for the RUNs 2009 and 2010. Simulated distributions of K^+K^- (ALICE approach). The red line is the K^+K^- distribution, the black line is the sum of K^+K^- and residual background. In the subsamples 70% and 30%, the residual background is small, and these two lines practically coincide.

Therefore, the experimental data will be analysed only in the ALICE and Martin approaches. The large residual background in the 50% subsample indicates that this experimental distribution is less reliable than in the other two subsamples.

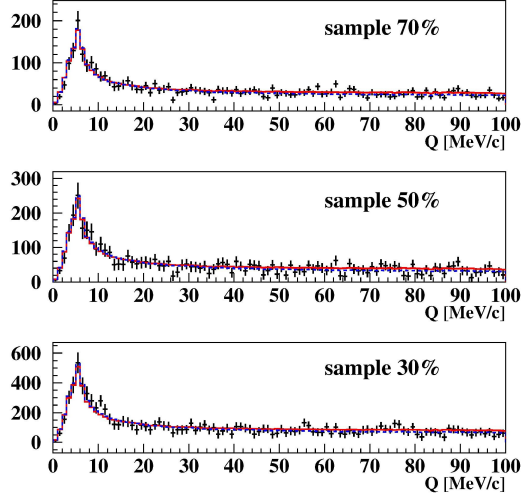


Fig. 4: Q distributions in the interval $0 - 100 \text{ MeV}/c$ of K^+K^- (ALICE approach) of the subsamples 30%, 50% and 70% for the RUNs 2009 and 2010 after residual background subtraction. The red and the blue fitting curves were evaluated by analysing the experimental distributions with residual background in the Coulomb and Martin approaches, respectively. The difference between these curves is not significant, and they describe well the "pure" experimental K^+K^- distributions.

Fig.3 shows the experimental distributions in Q , the fitting curves describing K^+K^- pairs (ALICE approach), residual backgrounds and the sum of the fitting curves and residual backgrounds. For the 70% (30%) subsample, the fitting curve alone describes well the experimental distribution in the total interval of Q , demonstrating that admixture of the residual background to the K^+K^- pairs is relatively small. This result is in agreement with the average level of the residual background, being equal to 3% (3.2%) of the total event number in the distribution. The same analysis was done for the 50% subsample where the residual background level is larger than that in the other two subsamples. The corrected experimental distribution (ALICE approach) was obtained after background subtraction and is shown in Fig.4. The red and the blue fitting curves in Fig.4 were evaluated by the analysis of the experimental distributions with residual background in the Coulomb and Martin approaches, respectively. The Martin fitting curve describes the corrected experimental distribution well. The small difference between the Martin and Coulomb approaches in the interval $30 - 100 \text{ MeV}/c$ is caused by the strong final state K^+K^- interaction taken into account only in the Martin approach. In Fig.5, the distributions in the interval $0 - 30 \text{ MeV}/c$ are presented. The Martin and Coulomb fitting curves, presented as histograms, coincide in this region and describe the corrected experimental data well. The efficiencies of all cuts are known. Using these efficiencies, the total numbers of detected K^+K^- pairs in the 70%, 50% and 30% subsamples were evaluated: 40890 ± 4110 , 29650 ± 3880 and 38140 ± 4430 pairs, respectively. The background in the 30% subsample is about 19 times larger than in the 70% subsample. Nevertheless, the total numbers of K^+K^- pairs are in good agreement demonstrating that the background and residual background subtraction was done correctly. The K^+K^- pair number in the 50% subsample differs from the other two values by two standard errors, confirming – as mentioned above – that the experimental data of this subsample are less reliable. The total number of K^+K^- pairs calculated in the Martin approach differs from the before quoted numbers (ALICE approach) significantly less than the presented errors.

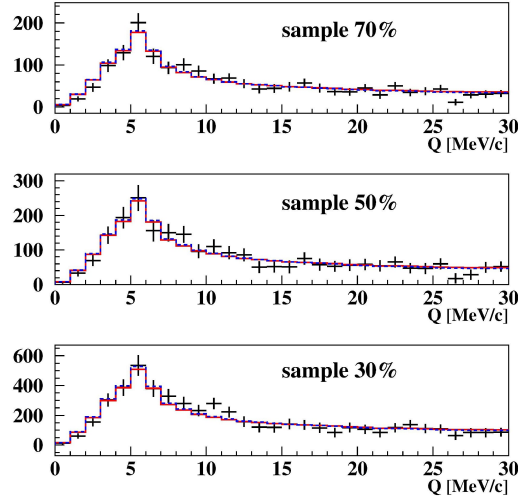


Fig. 5: Q distributions in the interval $0 - 30 \text{ MeV}/c$ of K^+K^- (ALICE approach) of the subsamples 30%, 50% and 70% for the RUNs 2009 and 2010 after residual background subtraction. The red and the blue fitting curves were evaluated from the analysis of experimental distributions with residual background in the Coulomb and Martin approaches, respectively. In this Q interval, there is no difference between these curves which describe well the “pure” experimental K^+K^- distributions.

1. The preprint draft on K^+K^- pairs will be sent to the Collaboration before November 2020. Before April 2021, the preprint will be submitted.
2. DIRAC plans to evaluate for the first time the number of K^+K^- atoms generated jointly with the detected K^+K^- pairs. The result will be submitted as a CERN preprint before October 2021.

2 Proton-antiproton pair analysis

The shape of the detected proton-antiproton pairs as a function of the relative momentum Q is expected to be more sensitive to the size of the particle production region as compared to K^+K^- pairs. Thus, the study of this shape could open a possibility to evaluate the size of the pair production region.

The pair distribution in Q will allow to evaluate for first time the number of relativistic proton-antiproton atoms generated jointly with the detected proton-antiproton pairs.

The investigation of the proton-antiproton system in the region of relative momentum from zero to $100 \text{ MeV}/c$ will be performed and the result be submitted as a CERN preprint before October 2021.

3 Short-lived $\pi^+\pi^-$ atom lifetime measurement

Previously, $\pi^+\pi^-$ pairs from the 2008-2010 data were used as calibration process for the πK and K^+K^- pair analysis. DIRAC expected to get a better statistics of $\pi^+\pi^-$ pairs compared to the already published result. Preliminary results on the measurement of the short-lived atom lifetime and $\pi^+\pi^-$ scattering lengths, basing on the new data, will be presented in October 2021.